SUPPLEMENTARY MATERIALS: Asymptotic, convergent, and exact truncating series solutions of the linear shallow water equations for channels with power law geometry*

Geir Pedersen †

SM1. Outline.

SM2 is related to section 4 of the main text and contains additional mathematical details and examples on waves in simple geometries defined by power functions. The subsection SM2.1 offers an explanation for why the asymptotic expansion (3.3) works better in deep water than in shallow water if $\alpha < 2$, and the other way around if $\alpha > 2$. Self-similarity of 3.3 for power function geometries is briefly described in SM2.2. Next, SM2.3 sketches the special amplitude recursion for $\alpha = 2$ that was omitted in 4.1, while the following SM2.4 discusses the qualitative properties of the trailing systems for ranges of α and β. SM2.5 then give examples complimentary to those of 4.4.

SM3 is intended to widen the scope of 5. First SM3.1 gives additional mathematical details on the modified recursion for a composite geometry with an apex. SM3.2 give additional solutions for non-planar slopes, linked to 5.2. Then SM3.3 presents the boundary value problem on a slope that is related to the apex problem. Finally, another type of channel geometry and amplitude recursion for the amplitudes in (3.3) is presented in SM3.4. This allows for a gradual transition between uniform and variable channel sections and reflections from the transition are identified.

In SM4 effects of approximated transmission on runup of sloping beaches are studied. In particular, one reason for a mild underestimation by the allegedly most famous runup formula is pointed out.

The numerics employed in the article is not of the advanced sort. Anyway, a brief description is found in SM5.

In addition to power function geometries also geometries defined through exponentials have been investigated. Key results are given in SM6.

The section SM7 relates the properties of the asymptotic expansions to the global balance of energy, mass and momentum. In particular the need for a trailing system is discussed and, at the same time, the lack of special properties of the closed form solutions with respect to conservation becomes apparent.

In the final section of the supplement, SM8, the well-posedness of the linear shallow water equations for the channel is discussed in terms of integrated error estimates.

SM2. Power function geometries; additional subtopics.

SM2.1. Channel variation rate relative to α.

As a measure of variation rate of the medium we may use the typical change of wave speed, $c = \bar{h}^{\frac{1}{2}}$, over a wavelength; $l_r = \lambda c^{-1} \frac{dc}{dx}$, where $\lambda \sim \kappa \bar{h}^{\frac{1}{2}}$ is a measure of the wavelength. Then $l_r \sim \text{const.} x^{-\mu}$ decreases and increases

*December 29, 2020

†Department of Mathematics, University of Oslo, PO box 1053, 0316 Oslo, Norway (geirkp@math.uio.no, https://www.mn.uio.no/math/english/).

with x for $\alpha < 2$ and $\alpha > 2$, respectively. We would then expect that the asymptotic approximation is best in deeper water for $\alpha < 2$, while the opposite should be the case for $\alpha > 2$. This is consistent with the observations on the optimal number of terms, $j_{\min}$, in the asymptotic expansions for $F_0 = Y_0$, as discussed at the end of section 4.3.1. It also agrees with the convergence rate of series for $F_0 = P_0^{(M)}$, as is given in (4.11).

SM2.2. Self-similarity of (3.3). The solution defined by (3.3) and (4.3) may be scaled such that $x_0 = h_0 = 1$ (see section 2). Similarity properties are then revealed by changing the reference position to x_1 and re-scaling according to $\bar{x} = x_1^{-1}x$ and $\bar{t} = x_1^{-\mu}(t - \tau(1) + \tau(x_1))$. Then the solution is retrieved as the same expression with $\bar{C}_0 = x_1^{-p}C_0$ and $\bar{\kappa} = x_1^{\mu}\kappa$. Hence, the depth reduction diminishes the "effective κ" when $\alpha < 2$, and increases it when $\alpha > 2$.

SM2.3. Explicit recursion for $\alpha = 2$. For $\alpha = 2$ (4.2) and (4.3) become invalid and A_j may no longer be expressed solely in terms of power functions. Instead a compact recursion is written as

$$A_j = x^{-\frac{1}{2}(\beta+1)} \sum_{n=0}^{j} a_n^{(j)} (\ln x)^n, \quad a_n^{(j)} = \frac{1}{2} h_0^{\frac{1}{2}} \left\{ \frac{(\beta+1)^2}{4n} a_{n-1}^{(j-1)} - (n+1) a_{n+1}^{(j-1)} \right\}. \tag{SM2.1}$$

Ambiguity is avoided by requiring $a_0^{(j)} = 0$ for $j > 0$. For $j = n$ only the first of the two terms within the curly brackets is retained (corresponding to defining $a_n^{(j)} = 0$ for $j > n$). The phase becomes $\Theta = \kappa(h_0^{-\frac{1}{2}} \ln(x/x_0) + t)$.

It is noteworthy that for a quadratic depth profile the wave equation (2.2) may be transformed to a Klein-Gordon equation, with constant coefficients [SM3]. Also the exact solutions for oscillations in a parabolic basin come to mind [SM9]. However, there is no apparent mathematical link between these solutions and (SM2.1).

SM2.4. The first order corrections. The most important qualitative features of the asymptotic solutions are defined by the first two terms of the expansions (3.3) and (3.7). In the present subsection we assume $\beta < 1$ for simplicity. When the $O(\kappa^{-1})$ amplitude factor for the velocity is defined as $U_1 \equiv -\bar{h}^{-\frac{1}{2}} A_1 + A_{0,x}$ (see eq. (3.7)), it follows from (4.2), and the definitions $\mu = 1 - \frac{1}{2}\alpha$ and $p = \frac{1}{4}\alpha + \frac{1}{2}\beta$, that

$$A_1 = C_0 \frac{p(\mu - p)}{2\mu} h_0^{\frac{1}{2}} x^{-p-\mu}, \quad U_1 = C_0 \frac{p(\mu + p)}{2\mu} x^{-p-1}. \tag{SM2.2}$$

For $\alpha < \frac{4}{3} - \frac{2}{3}\beta$ the principal wave is trailed by a wave system with an elevation and a positive particle velocity (opposite direction of the wave advance). They drain volume and energy from the principal wave during propagation (see sec. SM7.2). When $\alpha = \frac{4}{3} - \frac{2}{3}\beta$ the trailing elevation vanishes ($A_1 = 0$), but the fluid velocity remains ($U_1 \neq 0$). Accordingly, $\eta = A_0 F_0$ and $u = \bar{h}^{-\frac{1}{2}} A_0 F_0 + \kappa^{-1} U_1 F_1$ form an exact solution (see section 4.2.1 and [SM4]). For $\frac{4}{3} - \frac{2}{3}\beta < \alpha < 2$ (SM2.2) yields a trailing depression and a (still positive) fluid velocity which must counterbalance the formation of this depression in addition to the volume loss in the principal wave.

For $\alpha = 2$ and $\beta = 0$ a two term solution reads

$$\text{(SM2.3)} \qquad \frac{\eta}{C_0} \sim x^{-\frac{1}{2}} F_0 + \frac{h_0^{\frac{1}{2}}}{8\kappa} x^{-\frac{1}{2}} \ln x \, F_1, \quad \frac{u}{C_0} \sim -h_0^{-\frac{1}{2}} x^{-\frac{3}{2}} F_0 + \frac{1}{2\kappa} x^{-\frac{3}{2}} \left(\frac{1}{4} \ln x - 1 \right) F_1.$$

Here the trailing η and u both change sign, but at different locations. The exact positions of these are due to the manner the ambiguity in (SM2.1) was resolved for A_1 ($x_r = e^2$). The A_1 from (SM2.2) becomes infinite as $\alpha \to 2$. To reconcile (SM2.2) with (SM2.3) we must utilize the ambiguity in the amplitude recursion to replace $x^{\frac{\alpha}{4}-1}$ in the A_1 of the former with $x^{-\frac{\alpha}{4}}(x^{\frac{\alpha}{2}-1} - 1)$ before taking the limit. This corresponds to adding a $B^{-\frac{1}{2}} h^{-\frac{1}{4}}$ part to A_1 and thus redefine the principal wave shape (see discussion below (3.6)). As (SM2.2) stands, A_1 from this equation becomes large in the neighbourhood of $\alpha = 2$ which seems to question the validity of the approximations. However, as seen in section SM2.5 (SM2.2) may still be a valid start of an accurate solution, but additional terms must then be included.

Then, for $2 < \alpha < 4 + 2\beta$ the signs of the trailing u and the η are swapped as compared to $\alpha < 2$. When $\alpha = 4 + 2\beta$ (SM2.2) yields an exact solution again, this time with a velocity field defined by the principal wave alone, and a trailing system with a flat surface elevation. For $\alpha > 4 - 2\beta$ both u and the η are positive again.

SM2.5. Amplification of N-waves and on non-planar beaches.

For all examples in this subsection $\beta = 0$.

The N-wave is depicted in the upper panel of figure SM1. The tail is of higher order and is hardly visible. This may be described as a result of destructive interference between the tails from the crest and the trough. Otherwise the performance of the asymptotic approximation is rather similar to that for $F_0 = Y_0$.

As stated in section SM2.4 the higher A_j may become large when $\alpha \to 2$. For the example $\alpha = 1.95$, which is depicted in the lower panel of figure SM1, we observe that η_0 no longer defines the shape of the wave. Hence, the solution shown cannot be regarded as a modest perturbation of what is called the "principal wave". Still, if enough terms are retained the comparisons with numerical solutions show that the asymptotic series still provides a close approximation. In the lower panel of figure SM2 results for $\alpha = \alpha_5^{(ii)} = 20/9 = 2.222...$ and $F_0 = Y_0$ are depicted. Then η_5 is an exact solution. As for $\alpha = 1.95$ the deviations from η_0 are large, this time in form of an increased wave height and a high trailing surface elevation. When compared with solutions for similar, but slightly different, α values (not shown) the exact solutions, corresponding to the truncated series, do not appear to have any unique properties or to be distinguished in any way. For the limiting case of $\alpha = 2$ (upper panel) η_0 again presents the dominant part of the solution. Here $F_0 = P^{(4)}$ is the principal wave shape and the value of κ is reduced to have a rough match of wavelength with the other cases (see figure 2 in main article). It is stressed that the very different appearances for the α values close to 2 are linked to the differences in x_r in the recursion relation (3.6) for the amplitudes.

SM3. Waves entering the slope.

This section extends the scope on wave transmission to a slope. First transmission to non-planer beaches is presented. Among other things, the wave shapes of the transmitted waves are investigated and related to the strange shapes which were found in some cases in section SM2.5, as well as in figure 5 (main article). Then, a pulse is

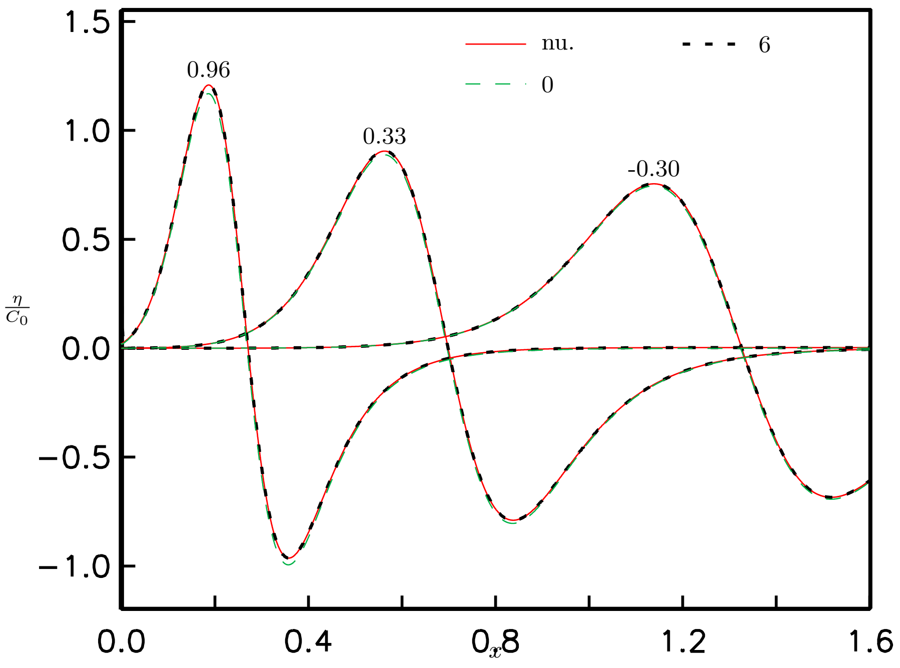

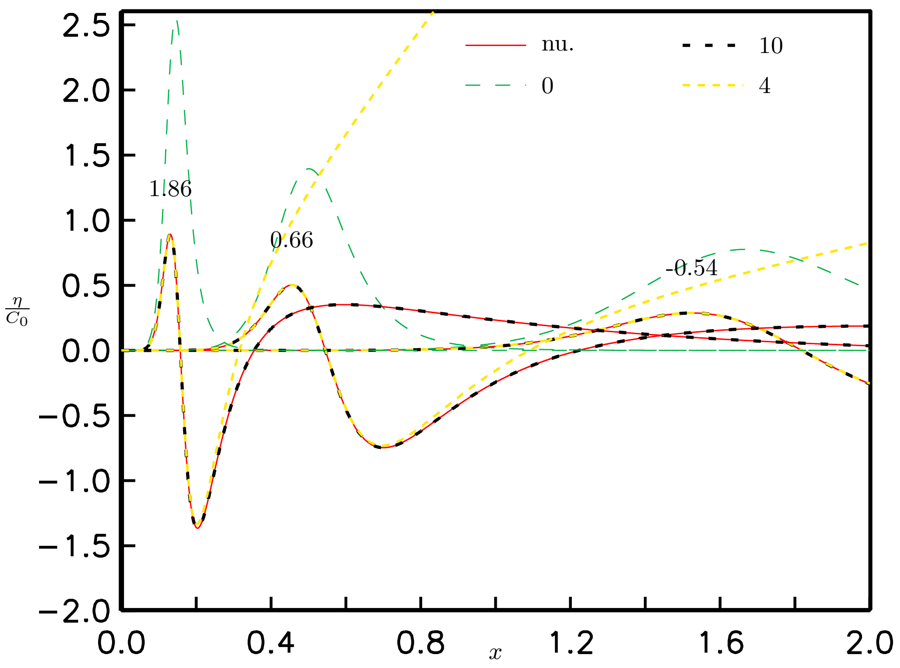

Figure SM1. *Numerical surface elevation and selected η_n at times as indicated above the crests. Upper panel: The N-wave ($F_0 = Y_{-1}$), $\kappa = 4$ $\alpha = 1$, and $t_0 = -1.57$. Lower panel: $F_0 = Y_0$, $\kappa = 4$ $\alpha = 1.95$, and $t_0 = -1.74$.*

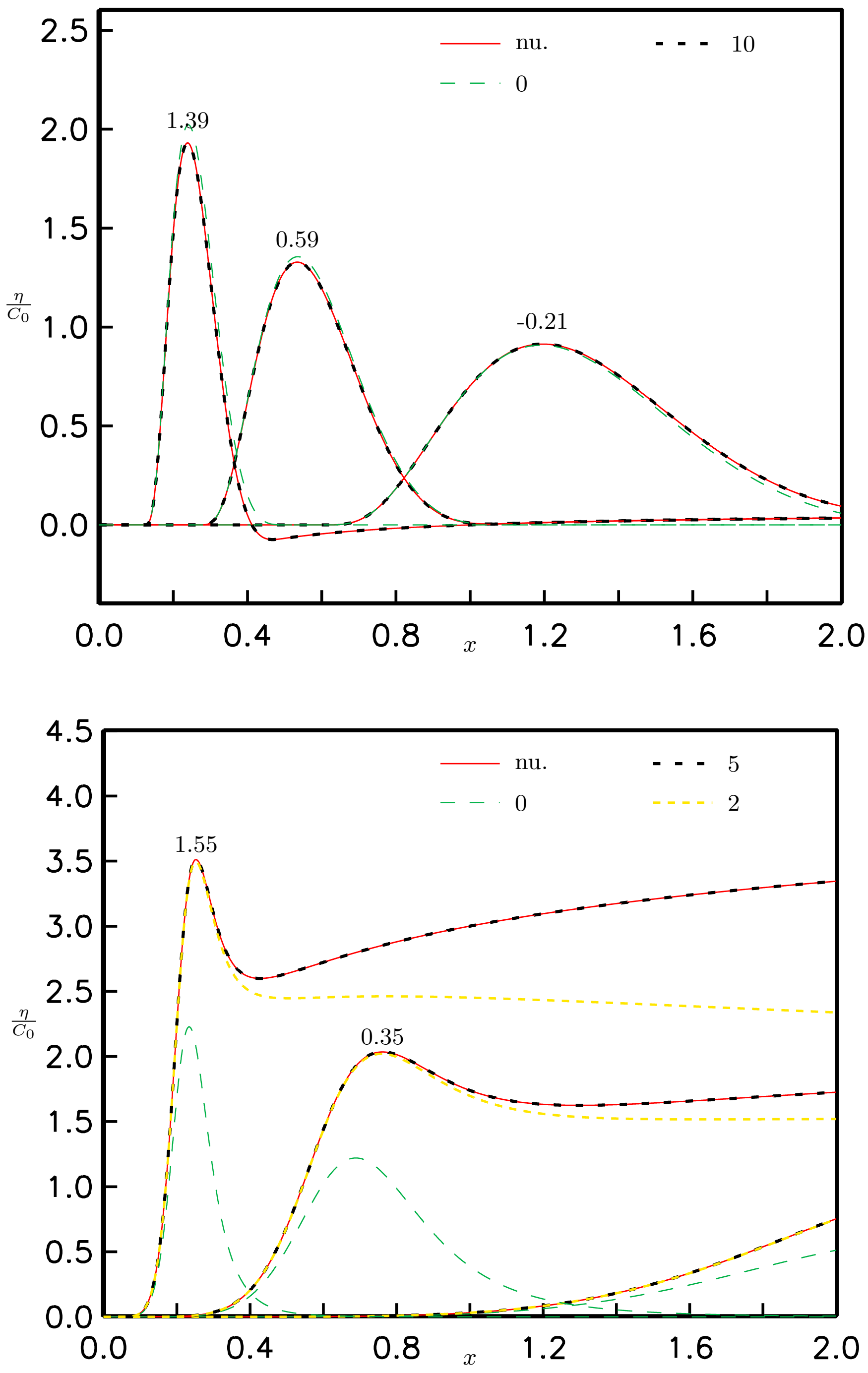

Figure SM2. *Surface elevations for selected beach profiles. Legends are as for figure SM1. Upper panel:* $F_0 = P_0^{(4)}$, $\kappa = 0.7$ $\alpha = 2$, *and* $t_0 = -1.41$. *Lower panel:* $F_0 = Y_0$, $\kappa = 3$, $\alpha = \alpha_5^{(ii)} = 2.222...$, *see (4.7), and* $t_0 = -2.05$.

simply generated from an input condition at a boundary located at the slope. The structure of the solution is quite similar to that of the wave transmitted through an apex. Finally, a new depth profile, with a smooth transition from a flat bottom to a slope, is investigated with special attention to reflections.

SM3.1. Amplitude recursion for waves transmitted at an apex or generated from the boundary. The amplitude recursion used for the transmission at an apex is $A_{j+1} = L(A_j)$ where the linear operator L is

$$L(v) = -\frac{1}{2}\bar{h}^{\frac{1}{2}}v' + \frac{1}{2}\sigma^{-2}A_0\int\limits_{x_0}^{x}\bar{h}BA_{0,x}v'd\hat{x}. \tag{SM3.1}$$

Next, we assume that $\bar{h}$ and B are polynomials for $x < x_0$. For $A_0 = \text{const.}\times x^{q_0}$, with $q_0 = -\frac{1}{2}\beta - \frac{1}{4}\alpha$, $L(A_0)$ will then be a combination of power q_1 and q_0. Another application of L will then give the three powers q_2, q_1 and q_0 etc. More specific

$$L(x^{q_n}) = \nu_n b_n x^{q_{n+1}} - (\nu_n b_n + \frac{1}{2}h_0^{\frac{1}{2}}q_n)x_0^{-(n+1)\mu}x^{q_0},$$

where, still, $\mu = 1 - \frac{1}{2}\alpha$ and ν_j, as well as b_j, are from (4.2). Normalizing this recursion formula by $C_0 = 1$ the form of A_j becomes

$$A_j = \sum_{n=0}^{j} a_n C_{j-n}x^{q_{j-n}}, \tag{SM3.2}$$

where C_j is still defined through the recursion (4.2). Here $a_0 = a$, provided the incident wave is aF_0, and the other amplitude factors are given by the recursion formula

$$a_j = -\sum_{n=1}^{j}\left(C_n + \frac{1}{2}h_0^{\frac{1}{2}}q_{n-1}C_{n-1}\right)x_0^{-n\mu}a_{j-n}. \tag{SM3.3}$$

SM3.2. Transmission through an apex to non-planar beaches.

SM3.2.1. The two term solution. With $\bar{h} = h_0x^\alpha$, $B = B_0x^\beta$ and $x_r = x_0$ an explicit modified recursion is outlined in section SM3.1. The amplitude of the second term becomes

$$A_1 = \begin{cases} \frac{1}{2}h_0^{\frac{1}{2}}\frac{x^{-p}}{x_0^{-p}}\left(\frac{p^2}{\mu}\left(x_0^{-\mu} - x^{-\mu}\right) + px^{-\mu}\right) & \text{if} \quad \alpha \neq 2, \\ \frac{1}{2}h_0^{\frac{1}{2}}\frac{x^{-p}}{x_0^{-p}}\left(p + p^2\ln\left(\frac{x}{x_0}\right)\right) & \text{if} \quad \alpha = 2, \end{cases} \tag{SM3.4}$$

where $\mu = 1 - \frac{1}{2}\alpha$ and $p = \frac{1}{4}\alpha + \frac{1}{2}\beta$. As stated in the main article the part of A_1 that is proportional to x^{-p} corresponds to a shape modification. For simplicity we now assume that α and β are both positive, which leads to $A_1(x_0) > 0$. However, $A_1(x)$ will change sign at some $x_s > 0$ when $\alpha > \frac{4}{3} - \frac{2}{3}\beta$. The position x_s increases (moves closer to the apex) with α and reaches $e^{-2(1+\beta)^{-1}}$ for $\alpha = 2$. Hence, the tail behind the principal wave may decrease in height but will become negative only in rather shallow water. In the case illustrated in SM4 a reduction in the height of the trailing wave is still hardly visible even when the front is near the shore. For $\alpha > 2$ the amplitude A_1 still starts out positive at $x = x_0$. As x decreases the shape-change part will dominate and A_1 becomes negative. There is no high trailing elevation, such as the one in the upper panel of figure SM2. An example for $\alpha = 3.7$ and $\beta = 0$ is shown in figure SM5.

SM3.2.2. Transmission for $\alpha = \alpha_0^{(i)}$. The reference [SM5] analyzed transmission from shallow to deeper water given by a $\alpha = \frac{4}{3}$ profile, using the Fourier transform, while the transmission at an apex in a parabolic channel was studied as a side problem in [SM7]. The latter is a special instance of the case in section 5.2.2. For $x < x_0$ the solution may we written as

$$\eta = x^{-\frac{\beta+1}{3}} H(\Theta),$$

where H is the unknown shape function. When (5.1) is still used for $x > x_0 = x_r$, patching of η and u and elimination of R yield

$$-\frac{\beta+1}{6\kappa} H + H' = I', \tag{SM3.5}$$

where the coefficients differ from those in [SM7] due to the general β and a different definition of the depth. Following [SM5] the solution of (SM3.5) can be written

$$H = e^{\frac{\beta+1}{6\kappa}\theta} \int_{-\infty}^{\theta} e^{-\frac{\beta+1}{6\kappa}s} I'(s) ds. \tag{SM3.6}$$

When an incident wave with compact support is assumed ($I = 0$ for $\Theta > \Theta_b$) the surface elevation at the apex becomes a constant times $e^{\frac{\beta+1}{6}t}$ for $\Theta(x_0, t) > \Theta_b$. The travel time from the apex to the beach and back again is $6/(\beta + 1)$, which is the e-folding time for η at the apex. Hence, the total growth is by a factor 3, say. The expansion (3.3) gave (5.7) which corresponds to (putting $A_0(x_0) = 1$)

$$H = \sum_{j=0}^{\infty} \left(\frac{\beta+1}{6\kappa}\right)^j F_j(\Theta), \quad F_0 = I. \tag{SM3.7}$$

Using the ratio criterion, as in section 4.3.2, we find convergence when I is a polynomial. The representation (4.9) of the front of the sech^2 shape ($I = Y_0$) yields convergence as long as β is of order 1 and κ is large. Presumably, (SM3.7) converges for wide classes of I, but we do not pursue this further herein. Then, substitution shows that (SM3.7) fulfills (SM3.5). Moreover, straightforward integration by parts on the integral in (SM3.6) shows that this expression coincides with (SM3.7) for $\Theta = \Theta_b$. Hence, (SM3.6) and (SM3.7) are equivalent.

The shape transformation and reflection for $\alpha = \frac{4}{3}$, $\beta = 0$ are illustrated in figure SM3.

SM3.3. Waves specified at a boundary.. A wave that propagates in the negative x-direction, for $x < x_0$, may be obtained as solution of a boundary value problem with $\eta(x_0, t) = I(\kappa t)$, where I is some shape function. To design an approximation we first choose the leading

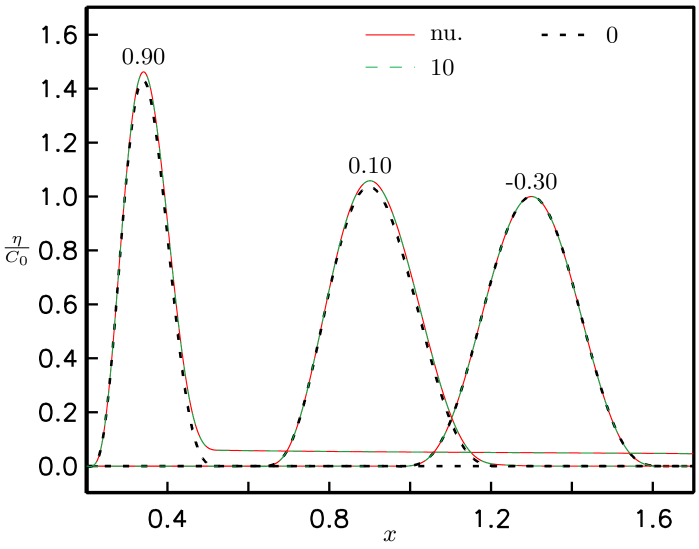

Figure SM3. *Normalized surfaces for transmission/reflection at an apex with* $\alpha = \frac{4}{3}$, $h_0 = x_0 = 1$, $\beta = 0$, $I = C_0 P_0^{(4)}$ *and* $\kappa = 1.5$. *The approximate solution* η_{10} *is compared to the numerical counterpart.*

order approximation according to $F_0 = I$ and $A_0 = B(x_0)^{\frac{1}{2}}\bar{h}(x_0)^{\frac{1}{4}}/B(x)^{\frac{1}{2}}\bar{h}(x)^{\frac{1}{4}}$. Then the free constant, x_r, in (3.6) is chosen independently for each j as to give $A_j(x_0) = 0$ for $j \geq 1$. This corresponds to a modification in the lower limit for the integral in (SM3.1) that yields a addition const. $\times\, \bar{h}^{-\frac{1}{4}}$ to A_{j+1} such that $A_{j+1}(x_0) = 0$. We then still have amplitudes on the form (SM3.2), but the second term within the parentheses of (SM3.3) vanishes.

As an example, after the normalization $h_0 = x_0 = 1$, the solution for a linear slope becomes

$$\eta \sim x^{-\frac{1}{4}}\left(F_0(\Theta) + \frac{1}{16\kappa}\left(x^{-\frac{1}{2}} - x^{-\frac{1}{4}}\right)F_1(\Theta) + \frac{1}{512\kappa^2}\left(9x^{-1} - 2x^{-\frac{1}{2}} - 7x^{-\frac{1}{4}}\right)F_2(\Theta) + \ldots\right).$$

Comparing with (4.14) we observe that a new shape modifying term is introduced in each negative power in κ (see discussion below (3.6)). A tail will then develop gradually as the wave moves away from the boundary and $x^{-\frac{1}{2}}$ will dominate $x^{-\frac{1}{4}}$.

SM3.4. A smooth transition from constant depth to a slope. When $\bar{h}(x)$ is a monotonic function it may be inverted, a least in principle, to give $x = x(\bar{h})$. Then, A_j and Θ may be expressed in terms of $\bar{h}$ rather than x. For simplicity we put $B = $ const., even though we could have introduced $B(\bar{h})$. It is now convenient to define

$$\frac{d\bar{h}}{dx} = G(\bar{h}). \tag{SM3.8}$$

With $A_j = A_j(\bar{h})$ the amplitude recursion (3.6) may then be rewritten

$$A_{j+1} = -\frac{1}{2}\bar{h}^{\frac{1}{2}}G(\bar{h})\frac{dA_j(\bar{h})}{d\bar{h}} - \frac{1}{8}\bar{h}^{-\frac{1}{4}}\int\limits_{\bar{h}_r}^{\bar{h}} s^{-\frac{1}{4}}G(s)\frac{dA_j(s)}{d\bar{h}}ds, \tag{SM3.9}$$

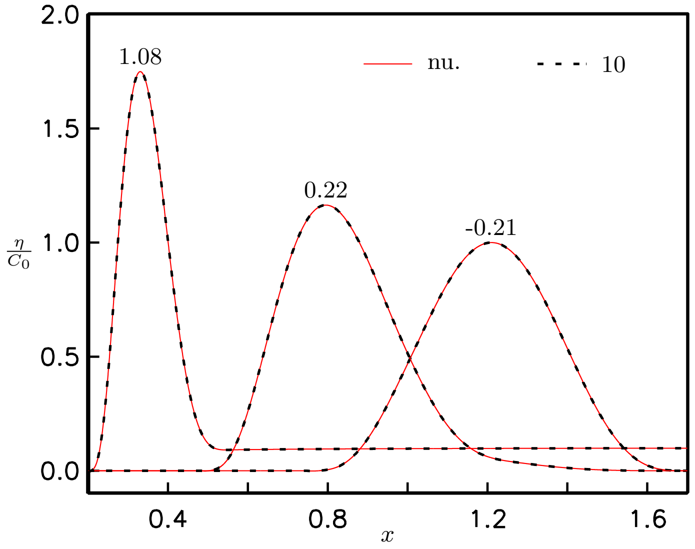

Figure SM4. *Normalized surfaces for transmission/reflection at an apex with* $\alpha = 1.95$*,* $h_0 = x_0 = 1$*,* $\beta = 0$*,* $I = C_0 P_0^{(4)}$ *and* $\kappa = 1.0$*. The approximate solution* η_{10} *is compared to the numerical counterpart.*

This new form of the recursion is easily solved in closed form when G is a power function. However, this will only reproduce the cases when $\bar{h}$ itself is a power function or an exponential.

On the other hand, if $G(0) = 1$ and $G \to 1$ as $\bar{h} \to 1$ equation (SM3.8) may yield a geometry that includes a beach at one end and a nearly flat bottom at the other. The choice $\bar{h}_r = 1$ in the recursion (SM3.9) makes all A_j, $j > 0$ vanish when $\bar{h} \to 1$. Then, for sufficiently small times the incident wave is given by F_0 alone, whereas a trailing wave system develops when the wave moves into the region with markedly decreasing depth. Simple examples of geometries with the desired properties are obtained with $G = 1 - \bar{h}^m$. A large m then gives a sharp transition, akin to an apex, whereas $m = 1$ and $m = 2$ give simple solutions also for the phase. When a shore is located at $x = 0$ the choice $m = 2$ leads to

$$G(\bar{h}) = 1 - \bar{h}^2, \quad \bar{h}(x) = \tanh(x). \tag{SM3.10}$$

The phase and A_1 then become

$$\Theta = \kappa\left(\arctan(\bar{h}^{\frac{1}{2}}) + \operatorname{arctanh}(\bar{h}^{\frac{1}{2}}) + t + D\right), \quad A_1 = \frac{1}{16}\bar{h}^{-\frac{3}{4}} + \frac{1}{12}\bar{h}^{-\frac{1}{4}} - \frac{7}{48}\bar{h}^{\frac{5}{4}}, \tag{SM3.11}$$

where D is a constant and the amplitudes are normalized such that A_0 becomes unity as $\bar{h} \to 1$. Also A_2 and A_3 are found as increasingly complex combinations of powers of $\bar{h}$. Logarithms appear in A_4 etc. and only results for $n \leq 3$ are investigated herein.

In figure SM6 we observe the amplification with decreasing depth and the evolution of the trailing system. For $n = 3$ both are described well within an error of 0.001 for $x < 1$ and $t < 1$. However, at the outskirt of the slope the deviations between numerical and analytical solutions increase after the passing of the wave and. At $t = 1$ the maximum deviation is

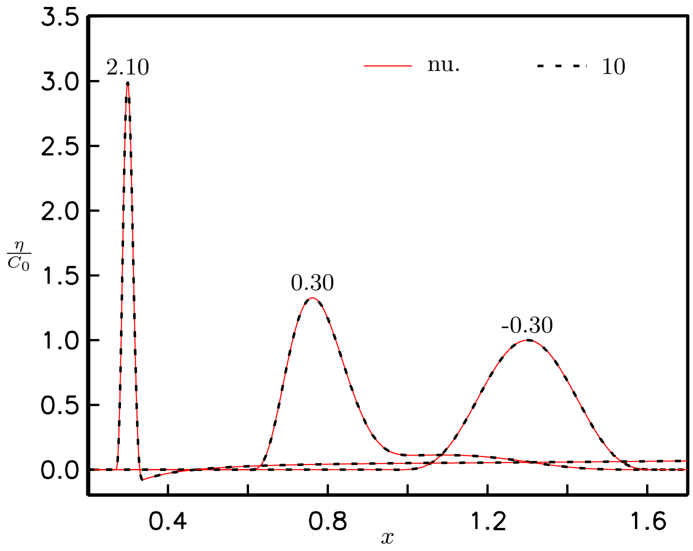

Figure SM5. *Normalized surfaces for transmission/reflection at an apex with* $\alpha = 3.7$*,* $h_0 = x_0 = 1$*,* $\beta = 0$*,* $I = C_0 P_0^{(4)}$ *and* $\kappa = 1.5$*. The approximate solution* η_{10} *is compared to the numerical counterpart.*

slightly above 0.004 while the error bound in (SM8.6) is as large as 0.033. Moreover, at this stage the lower panel of figure SM6 shows that the terms of (3.3) increase with n for $x > 3$, say. This indicates that the asymptotic expansion is inadequate, and not convergent by any rate, in this region. Anyway, the numerical solution evidently is a right-going wave for $x > 2.5$, say, which is not present in the expansion in this case. Since the wave still has not reached the shore at this time there is an apparent reflection from the geometry. Hence, the behaviour of (3.3) is qualitatively different in this case, as compared to the cases with geometries defined by powers (sec. 4.3.2) or exponentials (sec. SM6.3).

SM4. Transmission at the apex and maximum runup. At the shoreline, meaning $S = \bar{h}B = 0$ for a channel, the expansion (3.3) in general becomes invalid and runup at the shore cannot be calculated. On the other hand, the exact solutions, for which the series truncates, may be useful for runup analysis [SM2]. Still, the asymptotic approximation at the apex has some bearing on Synolakis' [SM8] simple and much celebrated formula for runup of solitary waves on an inclined plane.

The geometry and wave setup from section 5.2.1 (constant channel width and an inclined plane joined with a horisontal bottom) has been used in many theoretical and experimental investigations. One with particular impact is Synolakis' [SM8] study, which, among other things, contains a linear analysis of the runup an incident wave of the shape aY_0. The geometry is shown in figure SM7, together with a selection of incident waves from the subsequent analysis. In the [SM8] the application of a temporal Fourier transform led to an inversion integral involving Bessel functions. The transmission at the apex was simplified by the use of leading order asymptotic expressions for the Bessel functions. The linear runup solution was extended to a nonlinear solution by means of the hodograph transformation [SM1], with the

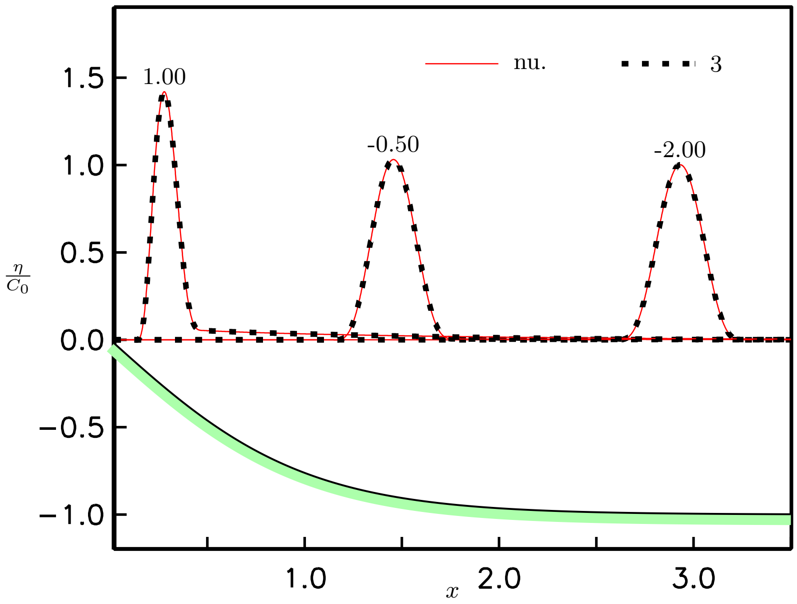

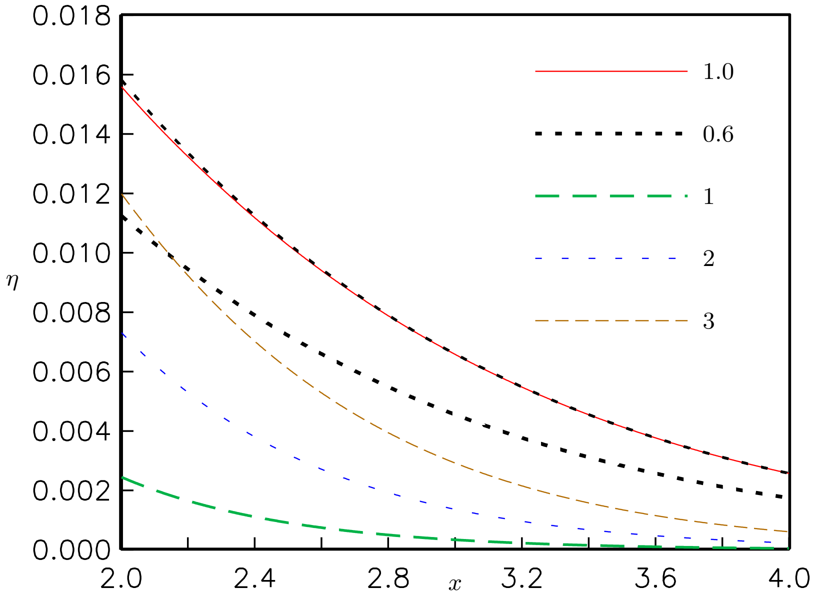

Figure SM6. *Selected results for $\bar{h} = \tanh x$, $F_0 = P_0^{(4)}$, $t_0 = -8$ and $\kappa = 1.5$. D is chosen according to $\Theta(1,0) = 0$. Upper panel: Geometry and surface elevation for three different times. Lower panel: Details for large x and t. Curves marked by times (floats) correspond to numerical solutions. The data for $t = 0.6$ are repeated with a 0.4 shift to the right, corresponding to the propagation of a reflected wave. For curves marked by integers the integers define the order of the asymptotic approximation, all for $t = 1.0$.*

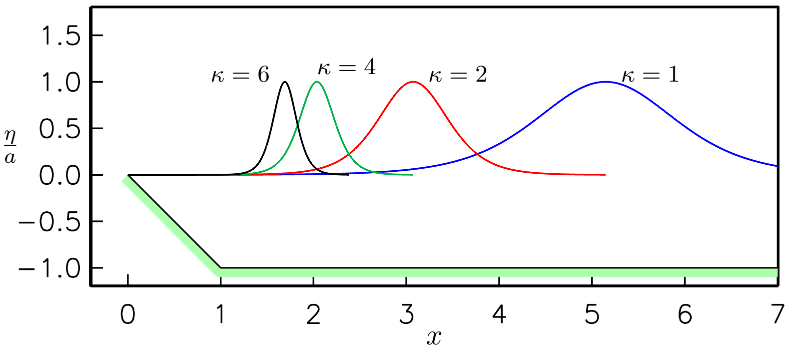

Figure SM7. *The wave tank geometry used in the sections 5.2 and SM4, together with incident waves $\eta = I = Y_0$ of different lengths.*

assumption that linear wave theory is valid well into the sloping region, but not necessarily close to the shore. Still, the maximum runup is the same as in the linear theory. In the original version of the runup formula the incident wave took on a solitary shape in the sense that $\kappa = \frac{1}{2}\sqrt{3a}$. Exploiting that the maximum runup height is proportional to a the formula is readily recasted into one where a and κ appear independently. When the maximum runup height is denoted by H_s the result of [SM8] then reads

$$\frac{H_s}{a} = 3.042\sqrt{\frac{\kappa}{h_0}}. \tag{SM4.1}$$

With $h_0 = 1$, and a slightly different notation from the reference, the first step toward (SM4.1) is patching of the local solutions

$$\eta = \begin{cases} A\mathrm{J}_0(2\omega\sqrt{x})e^{i\omega t} & \text{for } x \le 1, \\ ae^{i\omega(t+x-1)} + Re^{i\omega(t-x+1)} & \text{for } 1 \le x, \end{cases} \tag{SM4.2}$$

in the same manner as was done in section SM3.2.2. Here a is the amplitude of the incident harmonics, R the amplitude factor of the reflection and the solution on the plane is obtained by requiring $\eta(0,t)$ to be finite. The real parts of (SM4.2), say, has physical meaning. Using the leading asymptotics for J_0 and J_1 the result for A may be approximated, for large ω, according to

$$A = \frac{2a}{\mathrm{J}_0(2\omega) - i\mathrm{J}_1(2\omega)} \sim 2a\sqrt{\pi\omega}\, e^{i(2\omega - \frac{\pi}{4})} \tag{SM4.3}$$

The use of the rightmost expression is equivalent to invocation of the asymptotic approximations for the Bessel functions in the patching itself. The proceding steps of [SM8] correspond to using the approximate A, identifying $a(\omega)$ with the temporal Fourier transform of $Y_0(\kappa t)$, deforming the inversion integral in the complex plane and summing the resdiual contributions, albeit the approximations of the Bessel functions were introduced in a late stage in the reference. It is noted that the standard asymptotic series for $\mathrm{J}_0(2\omega\sqrt{x})$, multiplied with the temporal factor $\cos(\omega t)$, is reproduced by adding the asymptotic series (3.3), with $F_0 = \cos(\Theta)$, $\Theta = \omega(\tau(x)+t) - \frac{\pi}{4}$ and A_j defined from (4.2) with $C_0 = \frac{1}{2}\sqrt{2/\pi}$, and the corresponding series in (3.8) with $\hat{\Theta} = \omega(t - \tau(x)) + \frac{\pi}{4}$. In these series, that now are standard WKB series, ω takes the place of κ. The outline given above suggests that the use of the asymptotic approximation in [SM8], corresponds to solving the patching condition (5.2) only to leading order and, thus, employ the solution obtained from equation (4.2) as incident wave at $x = 1$ on an inclined plane. The numerical runup obtained from this boundary/initial condition is denoted $H_{\mathrm{a.p.N}}$, where N is the maximum number of terms (asymptotic series truncated at the smallest term). What is mainly lost in the formula (SM4.1) is then the effect of the shape change during the transmission as seen in, for instance, (5.5).

For comparison we solve the shallow water equations numerically with the formula (5.5), or its higher order counterparts, used for boundary conditions at $x = x_0$. The summation of (3.3) is stopped after the $O(\kappa^{-N})$ term or after the smallest one; whichever occurs first. This gives maximum runup heights which are denoted as H_N. For order $N = 0$ the incident wave produced in this manner will actually correspond to the expansion at the end of section SM3.3. We assume an effective wave-length equal to the distance between the two points where $Y_0 = 0.001$ and start the simulations at $t = t_i$, when the peak is half this length outside x_0 (the boundary of the computational domain). Since the solution (3.3) does not include reflections from the beach the maximum runup should be reached within $t - t_i = 6$, say, which is an estimate of the travel time from the apex to the beach, then back to the apex, and to the beach again. Provided $\kappa \geq 1$ it turns out that the maximum runup is reached before $t - t_i = 5.8$. Comparisons are made to *purely* numerical reference simulations with the incident wave specified as an initial condition out on the flat bottom part of the channel. The result, H_{num} then includes the full transmission. In addition we also make a “reasonably poorest attempt”, resulting in H_{poor}, by making simulations where the geometry is replaced by a single inclined plane and we start from rest with an elevation $\eta(x, 0) = 2aY_0(\kappa(x - 1))$.

The relative deviations from the reference solution,

$$\Delta H_* = \frac{H_{\mathrm{num}} - H_*}{H_{\mathrm{num}}},$$

are shown in table SM1 for a selection of κ values. It turns out that all the approximate solutions included undershoot the reference solution. Grid refinement tests point to an relative error in the results which is less than 10^{-4} for $\kappa = 6$ and which is smaller for the longer incident waves. As expected H_{poor} gives the largest error, while the error of H_0 is roughly half this size for the larger κ values. Then, H_1 is markedly better than H_0 as it takes the amplification in the transmission into account. Inclusion of the third term improves the agreement with the reference solution further and the relative deviation (ΔH_2) is less than 0.01 even for the long wave (see figure SM7) corresponding to $\kappa = 1$ and decreases to about 0.0001 for $\kappa = 4$. Keeping $\kappa = 1$ and increasing N, we find that ΔH_N first decreases and then changes sign at $N = 8$, before reaching an optimal value of -0.0005 for $N = 9$ (these values for ΔH_N are not included in the table). It must be noted that only a few terms are used for small times (front of wave being fed in), while the higher order terms only give useful contributions at larger times (see figure 3 in main article). The procedure leading to (SM4.1) takes into account all the wave evolution on the slope, but not the extra amplification due to the shape shift in

κ	$H_{\rm num}$	ΔH_0	ΔH_1	ΔH_2	ΔH_s	$\Delta H_{\rm a.p.10}$	$\Delta H_{\rm poor}$
1.0	3.241	0.1261	0.0250	0.0078	0.0614	0.0611	0.1457
1.5	3.881	0.0804	0.0098	0.0019	0.0399	0.0397	0.1292
2.0	4.433	0.0593	0.0052	0.0007	0.0296	0.0294	0.1070
3.0	5.374	0.0390	0.0022	0.0002	0.0196	0.0194	0.0757
4.0	6.175	0.0291	0.0012	0.0001	0.0147	0.0145	0.0578
5.0	6.883	0.0232	0.0008	0.0000	0.0117	0.0115	0.0466
6.0	7.525	0.0192	0.0005	0.0000	0.0098	0.0096	0.0391

Table SM1

The relative runup height deviations ΔH_*, as defined in the text. The numbers refer to the orders included in (5.5) for the boundary forcing. ΔH_s corresponds to the result for Synolakis' runup formula (SM4.1), while the subscript poor *refers to the initial value problem on an inclined plane.*

the transmission at the apex. Hence, it is to be expected that ΔH_s falls between ΔH_0 and ΔH_2, as it neatly does. Moreover, $\Delta H_{\rm a.p.10}$, for which the shape modification at the apex is neglected, but a high order asymptotic solution is used as incident wave, is very close to ΔH_s.

Runup computations are made also for the geometry $h(x) = \tanh(x)$. Maximum runups are only slightly higher than for the apex geometry and the relative difference is decreasing with κ. For $\kappa = 1$ the difference is 1.7 %.

SM5. Numerical details.

SM5.1. Numerical solutions of the wave equation. Herein, the single equation (2.2), in its conservative form, has been solved by centered differences (a standard five point star-scheme) in space and time. Numerical solutions are mainly used for comparison with the analytic ones. In section SM4 it also used for runup on an inclined plane. Some extra care is then needed, by placing the shoreline midway between two spatial nodes and invoking the zero volume flux condition $B\bar{h}\eta_x = 0$ at this point. This both excludes the solutions that are singular at the shoreline and removes the need for an auxiliary node on-shore. Still, a fine grid is needed in shallow depths and grid refinement are performed for the computed cases.

SM5.2. Numerical integration of shape functions. Presumably a fair number of shape functions may be computed by direct successive integration with high order and fine resolution. However, a procedure that only integrates numerically expressions that are available in formulas is preferred. The integration is started at some negative value Θ_a, where (4.9) is used if $F_0 = Y_0$, but where all F_j is put to zero if such an expansion for large, negative Θ is unavailable. In the latter case Θ_a must have a sufficiently large absolute value. Then the shape functions are advanced from Θ_i to $\Theta_{i+1} = \Theta_i + \Delta\Theta$, say, by Taylor's formula on the form

$$F_j(\Theta_{i+1}) = \sum_{n=0}^{j-1} \frac{\Delta\Theta^n}{n!} F_{j-n}(\Theta_i) + \int_{\Theta_i}^{\Theta_{i+1}} \frac{(\Theta_{i+1} - \hat{\Theta})^{j-1}}{(j-1)!} F_0(\hat{\Theta}) d\hat{\Theta}, \qquad \text{(SM5.1)}$$

where the last term is integrated numerically by a Gaussian quadrature of high order (typically 14). First, $F_0(\Theta_{i+1})$ is calculated by its formula and then the F_j are found sequentially by

(SM5.1) until the desired degree of the expansion is reached. In this manner a table of values for F_n is computed and can then be interpolated by cubic splines to provide values for any given argument. Naturally, (SM5.1) may be employed for any shape function that vanishes sufficiently fast, e.g. exponentially, as $\Theta \to -\infty$.

SM6. Channel width and depth given by exponentials.

SM6.1. Amplitude recursion. Explicit expressions for amplitudes are also found when the geometry is described by exponentials

$$\bar{h} = h_0 e^{\alpha x}, \quad B = B_0 e^{\beta x}, \quad A_j = C_j e^{q_j x}. \tag{SM6.1}$$

Insertion of these expressions in (3.6), with $x_r = 0$ for $\alpha > 0$ and $x_r = \infty$ for $\alpha < 0$, yields

$$q_j = -\frac{1}{2}\beta + (\frac{1}{2}j - \frac{1}{4})\alpha, \quad C_{j+1} = -\frac{h_0^{\frac{1}{2}} q_j(q_j + \beta + \alpha)}{(j+1)\alpha} C_j. \tag{SM6.2}$$

This is only valid when $\alpha \neq 0$.

SM6.2. Exact solutions for geometries defined by exponentials. As for power functions we obtain two classes of α values for which the series (3.3) for η truncates after n terms. From (SM6.2) it follows

$$\alpha_n^{(i)} = \frac{-\beta}{n + \frac{3}{2}}, \quad \alpha_n^{(ii)} = \frac{\beta}{n - \frac{1}{2}}. \tag{SM6.3}$$

The first sequence requires that the width and the depth of the channel are increasing in different directions while the latter sequence allows for channels that become shallower and narrower in the same direction, provided $n > 0$. The special case $\alpha_0^{(ii)}$ corresponds to $B\bar{h}^{\frac{1}{2}} =$ const. When $\beta > 0$, $B\bar{h}^{\frac{1}{2}}$ is otherwise increasing with x for both families, implying that principal wave is amplified during propagation towards decreasing x.

SM6.3. Convergence properties. For exponential $\bar{h}$ a measure of the relative variation of the medium (see section SM2.1) becomes $l_r = \lambda c^1 \frac{dc}{dx} = \text{const.} \times e^{\frac{1}{2}\alpha x}$, meaning that the asymptotic expansion is better for the smaller x. This points to a behaviour of the series akin to that for polynomial $\bar{h}$ with a power larger than 2.

As $j \to \infty$ the ratio C_j/C_{j-1} from SM6.2 approaches $-\frac{1}{4}h_0^{\frac{1}{2}}\alpha j$. Invoking polynomial wave shapes we combine this with (A.4) and find, in analogy to (4.10), that the series (3.3) converges if

$$K \equiv \frac{|\alpha|}{4\kappa} h_0^{\frac{1}{2}} e^{\frac{1}{2}\alpha x}(\Theta - \Theta_0) < 1, \tag{SM6.4}$$

and diverges if $K > 1$. Introducing the shoreline position, x_f, as in section 4.3.2, we find

$$K = \frac{1}{2}\left|1 - e^{\frac{1}{2}\alpha(x - x_f)}\right| < 1. \tag{SM6.5}$$

Hence, when $\alpha > 0$ there is convergence in a region defined by $\bar{h} < 9\bar{h}(x_f)$ or $x - x_f < \alpha^{-1} 2 \ln 3 \approx 2.2\alpha^{-1}$.

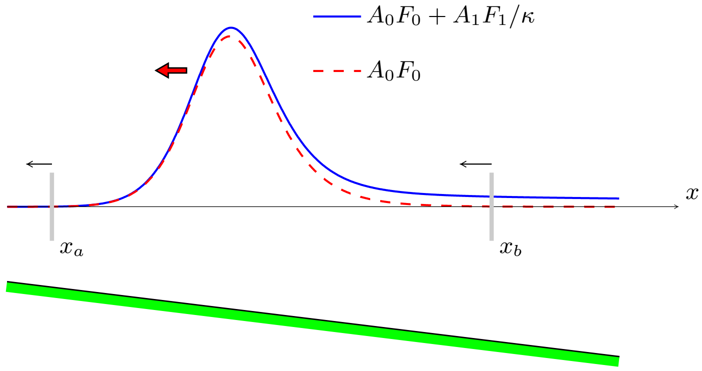

Figure SM8. *Definition sketch. The moving control volume for the balance of energy, mass and momentum.*

SM7. Conservation properties.

A general conservation equation reads

$$\frac{\partial T}{\partial t} = -\frac{\partial Q}{\partial x} + \mathcal{S}, \tag{SM7.1}$$

where T, Q and S are density, flux and source density, respectively. From the set (2.1) we readily obtain

	T	Q	$\mathcal{S}$
Energy	$\frac{1}{2}B\bar{h}u^2 + \frac{1}{2}B\eta^2$	$B\bar{h}u\eta$	0
Momentum	$B\bar{h}u$	$B\bar{h}\eta$	$\eta(B\bar{h})_x$
Volume	$B\eta$	$B\bar{h}u$	0

The momentum source term arises from the additional pressure, due to the surface elevation, on the channel perimeter.

It is now assumed that the shape function F_0 either has compact support or is vanishing exponentially at its outskirts. We may then identify the principal (leading order) wave as being confined to the interval $x_a(t) < x < x_b(t)$, where x_a is in front of the (left-propagating) wave system, while $\Theta(x_b, t)$ equals a sufficiently large constant value, Θ_b. It follows that $\frac{dx_b}{dt} = -\left(\bar{h}(x_b)\right)^{\frac{1}{2}}$. Integrating (SM7.1) over the interval we obtain

$$\frac{d\hat{T}}{dt} - \hat{\mathcal{S}} = -\left(Q + \bar{h}^{\frac{1}{2}}T\right)|_{x=x_b} \equiv -\mathcal{Q}_b, \quad \hat{T} = \int_{x_a}^{x_b} T dx, \quad \hat{\mathcal{S}} = \int_{x_a}^{x_b} \mathcal{S} dx, \tag{SM7.2}$$

where $\mathcal{Q}_b$ is the flux through the moving boundary $x = x_b$ and where we have exploited that Q and T are both zero at $x = x_a$. Equation (SM7.2) expresses the balance of the quantities in a moving domain as depicted in figure SM8.

Inserting the asymptotic series in $\hat{T}$ and $\hat{\mathcal{S}}$ we must deal with integrals that are of the type

$$I = \int_{x_a}^{x_b} f(x)G(\Theta)dx,$$

where f is some combination of amplitudes (A_j), $\bar{h}$ and B and where G is a linear or quadratic expression in the form functions (F_j). Moreover, we assume that G vanishes at $x = x_a$. I may be expanded by integration by parts

$$\text{(SM7.3)} \quad \begin{aligned} I &= \int_{x_a}^{x_b} f(x)G(\Theta)dx = \frac{1}{\kappa}\left(\bar{h}^{\frac{1}{2}}f\right)|_{x=x_b}G_1(\Theta_b) - \frac{1}{\kappa}\int_{x_a}^{x_b}\frac{d}{dx}\left(\bar{h}^{\frac{1}{2}}f\right)G_1 dx \\ &= \left[\frac{1}{\kappa}\bar{h}^{\frac{1}{2}}fG_1 - \frac{1}{\kappa^2}\bar{h}^{\frac{1}{2}}\frac{d}{dx}\left(\bar{h}^{\frac{1}{2}}f\right)G_2\right]_b + \frac{1}{\kappa^2}\int_{x_a}^{x_b}\frac{d}{dx}\left(\bar{h}^{\frac{1}{2}}\frac{d}{dx}\left(\bar{h}^{\frac{1}{2}}f\right)\right)G_2 dx, \end{aligned}$$

where $G_1 = \int_{-\infty}^{\Theta} G(s)ds$, etc., and the subscript, b, at the bracket indicates that the content is evaluated for $x = x_b$ and $\Theta = \Theta_b$. The process of integration by parts may be continued to any power in $1/\kappa$.

In the following we assume that the principal wave have a net volume in the sense that $F_1(\Theta_b) \approx F_1(\infty)$ is non-zero.

SM7.1. Energy conservation. Now $T = E = E_k + E_p$ where E_k and E_p are kinetic and potential energy, respectively. Inserting the asymptotic series in the densities and employing (SM7.1) we obtain a sum of products of factors of two different kinds. The first ones are expressions in terms of $\bar{h}$ and A_j, evaluated at $x = x_b$, whereas the second factors are expressions of $F_j(\Theta)$, or integrals of such, evaluated at $\Theta = \Theta_b$. Since Θ_b is constant only the first type of factors are differentiated when $\frac{d\hat{T}}{dt}$ is formed. When the two first orders are included, $\hat{E}_p$ and $\hat{E}_k$ become

$$\text{(SM7.4)} \quad \begin{cases} \hat{E}_p \sim \frac{1}{2\kappa}B\bar{h}^{\frac{1}{2}}A_0^2\int_{-\infty}^{\infty}(F_0(\Theta))^2 d\Theta + \frac{1}{2\kappa^2}B\bar{h}^{\frac{1}{2}}A_0A_1(F_1(\infty))^2 + O(\kappa^{-3}), \\ \hat{E}_k \sim \hat{E}_p + \frac{1}{2\kappa^2}B\bar{h}^{\frac{1}{2}}A_0A_{0,x}(F_1(\infty))^2 + O(\kappa^{-3}), \end{cases}$$

where A_j and $\bar{h}$ are evaluated at x_b. The leading order (κ^{-1}) contributions are constant due to (3.4) (Green's law). The next order (κ^{-2}) is different for kinetic and potential energy; the principle of energy equipartiton does not apply in non-uniform media. When the wave amplifies during propagation (toward decreasing x) we have $\hat{E}_k < \hat{E}_p$. Using the amplitude recursion formula in (3.5) we find the energy shedding rate

$$\text{(SM7.5)} \quad \frac{d\hat{E}}{dt} \sim -\frac{1}{2\kappa^2}B\bar{h}^{\frac{3}{2}}(A_{0,x})^2(F_1(\infty))^2 = -\frac{1}{8\kappa^2}\bar{h}\left(\frac{\bar{h}_x}{2\bar{h}} + \frac{B_x}{B}\right)^2(F_1(\infty))^2,$$

which implies that the principal wave looses energy to the trailing system whenever there is amplification or attenuation. The expression is akin to the formula first reported by [SM6] for the energy loss of a solitary wave over an uneven bottom. Equation (SM7.5) may be checked by direct calculation of $-\mathcal{Q}_b$, which gives the same result. If the volume of the principal wave is zero ($F_1(\infty) = 0$) the energy loss of the principal wave will be of higher order, corresponding to the trailing wave system being of higher order.

According to (SM7.5) the rate of energy loss in the principal wave, due to the trailing system, depends explicitly on relative rates of change of B and $\bar{h}$. Hence, in this respect there is no difference between the exact truncated solutions and others. However, this only applies as long as the asymptotic approximation is valid.

SM7.1.1. Energy balance in power geometries. When the geometry is defined through power functions the energy shedding rate and fluxes become

$$Q \sim \gamma(x_b)\frac{p^2}{4\mu^2}(p^2 - \mu^2), \quad \frac{d\hat{E}}{dt} \sim -\frac{1}{2}\gamma(x_b)p^2, \quad \bar{h}^{\frac{1}{2}}E \sim -\left(\frac{d\hat{E}}{dt} + Q\right), \tag{SM7.6}$$

where

$$\mu = 1 - \frac{1}{2}\alpha, \quad p = \frac{1}{2}\beta + \frac{1}{4}\alpha, \quad \gamma(x) = \kappa^{-2}B_0 h_0^{\frac{3}{2}} C_0^2 [F_1(\infty)]^2 x^{\alpha-2}.$$

From figure SM9, left panel, we observe that the energy increase in the trailing system, represented by $\bar{h}^{\frac{1}{2}}E$, is more important for the energy shedding of the principal wave than the flux, Q. The latter is zero for $\alpha = \alpha_0^{(i)}$ and becomes negative (transport in the direction of wave advance) when $\alpha > \alpha_0^{(i)}$. The relative energy loss when the tail moves from $\bar{h}(1) = h_0$ to $h_b = \bar{h}(x_b)$ is

$$\hat{e} \sim \frac{\int\limits_{x_b}^{1} \frac{d\hat{E}}{dt}\bar{h}^{-\frac{1}{2}}dx}{\frac{1}{2\kappa}B\bar{h}^{\frac{1}{2}}A_0^2 \int\limits_{-\infty}^{\infty}(F_0(\Theta))^2 d\Theta} = \frac{h_0^{\frac{1}{2}}p^2}{2\kappa\mu}\left(\frac{[F_1(\infty)]^2}{\int\limits_{-\infty}^{\infty}(F_0(\Theta))^2 d\Theta}\right)\left(x_b^{-\mu} - 1\right). \tag{SM7.7}$$

For $F_0 = Y_0$ the parenthesis in the middle of the right expression becomes 3. The right panel of figure SM9 shows that $\hat{e}$ has a minimum for an $\alpha = \alpha_m$ that decreases with h_b. Concerning energy loss in the principal wave there is again nothing that distinguishes the exact solution with $\alpha = \alpha_0^{(i)}$.

SM7.2. Volume conservation. For volume the relative change in $\hat{T}$ is of lower order than the change in the energy. Hence, a leading order expression is obtained from $\eta \sim A_0F_0$, alone. The use of (3.4) then yields the compact result

$$\frac{d\hat{T}}{dt} \sim \kappa^{-1}B\bar{h}A_{0,x}F_1(\infty), \tag{SM7.8}$$

which implies that a wave amplifying while propagating to the left needs to shed volume. From (SM7.2) it then follows

$$-\kappa^{-1}B\bar{h}A_{0,x}F_1(\infty) \sim \mathcal{Q}_b = B\bar{h}^{\frac{1}{2}}(\eta + \bar{h}^{\frac{1}{2}}u)|_{x=xb}, \tag{SM7.9}$$

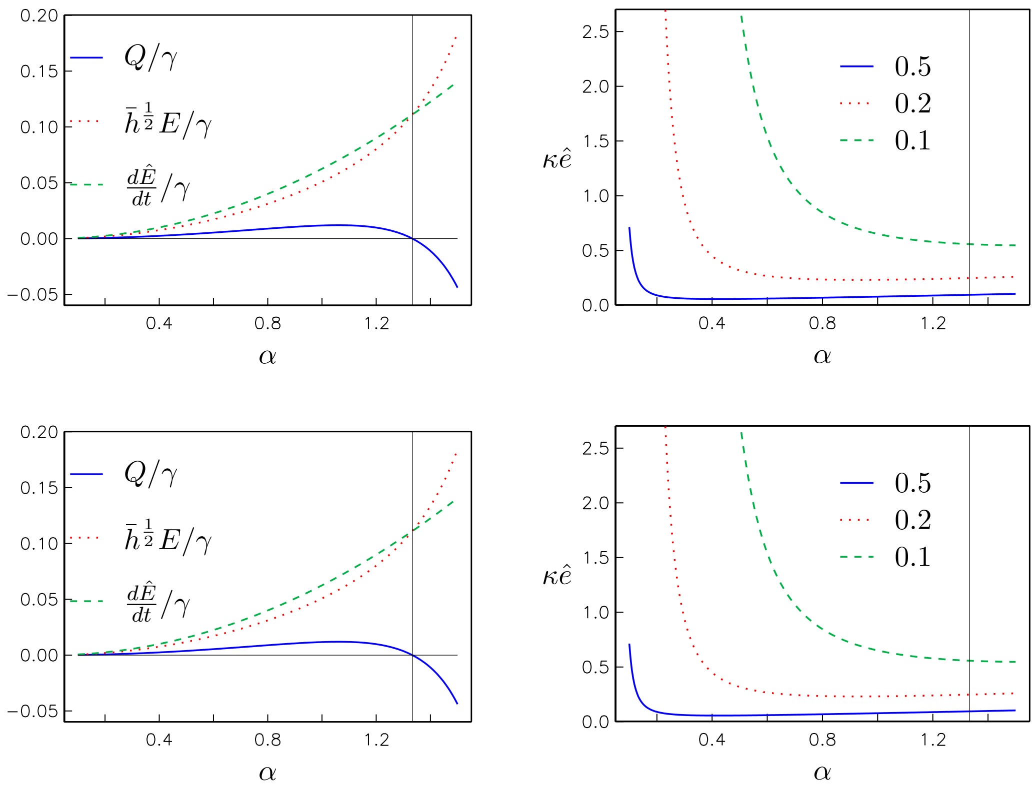

Figure SM9. *Results for $\beta = 0$ and $F_0 = Y_0$. Left: Relative importance of energy loss factors. Right: relative energy loss in principal wave from $h = h_0$ to $h = h_b$. Curves marked with value of h_b/h_0.*

which expresses that volume in the leading pulse is removed by a combination of a prolongation of a trailing surface elevation (first term within the parentheses) and a fluid velocity (second term). While the sum of these contributions is determined by $B\bar{h}A_{0,x}$, they may be unequal and even of different signs (see sec. SM2.4). When the series (3.3) and (3.7) are inserted on the right hand side of (SM7.9) the leading order terms (κ^0) cancel out and the next order terms combine to equal the left hand side.

SM7.3. The balance of horizontal momentum. For the momentum (SM7.2) yields the same equation as for the volume conservation, save that each term is multiplied by $\bar{h}^{\frac{1}{2}}$. However, the interpretations of some of the terms are quite different. The momentum of the principal wave is negative and decreases in magnitude, such that

$$\frac{d\hat{T}}{dt} \sim \kappa^{-1}\bar{h}^{\frac{1}{2}}(B\bar{h}A_0)_x F_1(\infty),$$

is positive when $B^{\frac{1}{2}}\bar{h}^{\frac{3}{4}}$ increases with x. The increase is provided by the sidewall/bottom source term, $\hat{\mathcal{S}}$. However, this term produces a surplus positive momentum, making $\frac{d\hat{T}}{dt} - \hat{\mathcal{S}}$ positive. This extra positive momentum is then carried away by the trailing fluid velocity and surface elevation in $\mathcal{Q}_b$. This may be concieved as a form of reflection, even though it is not conveyed by something that immediately can be recognized as a traveling wave. Momentum balance also leads to (SM7.9).

SM7.4. Energy transmission at an apex. As pointed out in section 5.1 the first order amplitude in the transmission of an elevation wave, A_1, becomes positive when the wave is amplifying in the variable part of the channel after the apex. This may be reconciled with energy conservation due to the reduced kinetic energy in (SM7.4). When the incident wave is defined by I it's energy becomes $E_i = \kappa^{-1}\int_{-\infty}^{\infty}(I(\Theta))^2 d\Theta$. According to (3.4) and (SM7.4) the energy immediately after transmission (the whole of I has passed x_0) is

$$\hat{E} \sim E_i + \frac{1}{4}\kappa^{-2}\left(A_0(x_0)\right)^{-1} A_{0,x}(x_0)\left(\int\limits_{-\infty}^{\infty} I(\Theta)d\Theta\right)^2.$$

Hence, even though the wave height of the transmitted wave is larger than that of the incident wave, the energy is smaller. The difference then goes into the reflected wave.

SM8. Error estimate for the boundary value problem.

A boundary value problem is defined on an interval $x_a \le x \le x_b$ by combining (2.1) with $\eta = \eta_n$ and $u = u_n$ as initial conditions and $\eta = \eta_n$ used for the boundary conditions at $x = x_a$ and $x = x_b$. Here, η_n and u_n are the partial sums from (3.3) and (3.7), respectively, including the terms of order κ^{-n}. If u is eliminated from this system we obtain the boundary value problem given at the start of section 4.4. The errors are then $v = u - u_n$ and $\zeta = \eta - \eta_n$. The error ζ corresponds to $\Delta\eta_n$ from section 4.4. The errors are solutions of the modified boundary value problem

$$v_t = -\zeta_x - r_n, \quad B\zeta_t = -(B\bar{h}v)_x - R_n, \tag{SM8.1}$$

with the boundary conditions $v = \zeta = 0$ at $t = 0$ and $\zeta = 0$ at $x = x_a, x_b$. The residuals, r_n and R_n, are found by substituting u_n and η_n into (2.1). Multiplying the momentum part of (SM8.1) with $B\bar{h}v$, integrating over the interval and using $\zeta = 0$ at $x = x_a, x_b$ we obtain the energy-type equation

$$\frac{d}{dt}\left[\epsilon\right] = -\left[R_n\zeta\right] - \left[B\bar{h}r_n v\right], \tag{SM8.2}$$

where $\epsilon = \frac{1}{2}B\zeta^2 + \frac{1}{2}B\bar{h}v^2$ and $[f]$ is the average of f over the solution interval (integral from x_a to x_b divided by $x_b - x_a$). Spatial extrema over the interval are marked by the indices 'max' and 'min' and auxiliary inequalities read

$$[\epsilon] \ge \frac{1}{2}B_{\min}\left[\zeta^2\right], \quad [\epsilon] \ge \frac{1}{2}(B\bar{h})_{\min}\left[v^2\right], \quad \left[f^2\right] \ge \left([|f|]\right)^2. \tag{SM8.3}$$

The combination of (SM8.2) and (SM8.3) leads to

$$\frac{d}{dt}\left[\epsilon\right] \le \sqrt{2}\,\gamma\sqrt{[\epsilon]}, \quad \gamma = \frac{|R_n|_{\max}}{\sqrt{B_{\min}}} + \frac{|B\bar{h}r_n|_{\max}}{\sqrt{(B\bar{h})_{\min}}}. \tag{SM8.4}$$

By use of the initial conditions this expression is readily integrated to

$$\sqrt{[\epsilon]} \leq \frac{1}{\sqrt{2}} \int_0^t \gamma dt, \tag{SM8.5}$$

which again implies the following error estimate for the surface elevation

$$\sqrt{[\zeta^2]} \leq \frac{1}{\sqrt{B_{\min}}} \int_0^t \gamma dt, \tag{SM8.6}$$

where the left hand side is recognized as the normalized L_2 norm from section 4.4.

Insertion of the expressions for u_n and η_n followed by application of the recursion formula for the amplitude yield

$$r_n = \kappa^{-n} A_{n,x} F_n, \quad R_n = B\bar{h}^{\frac{1}{2}} r_n.$$

Through the elimination of u these are shown to be fully compatible with the residue

$$-\kappa^{-n} B^{-1} (B\bar{h} A_{n,x})_x F_n$$

for the second order equation for η, (2.2).

REFERENCES

[1] G. F. Carrier and H. P. Greenspan, *Water waves of finite amplitude on a sloping beach*, J. Fluid Mech., 4 (1958), pp. 97–109.

[2] I. Didenkulova and E. Pelinovsky, *Nonlinear wave evolution and runup in an inclined channel of a parabolic cross-section*, Physics of Fluids, 23 (2011), p. 086602.

[3] I. Didenkulova and E. Pelinovsky, *On shallow water rogue wave formation in strongly inhomogeneous channels*, Journal of Physics A: Mathematical and Theoretical, 49 (2016), p. 11pp, https://doi.org/10.1088/1751-8113/49/19/194001.

[4] I. Didenkulova, E. Pelinovsky, and T. Soomere, *Long surface wave dynamics along a convex bottom*, J. Geophys. Res., 114 (2009), pp. 2156–2202.

[5] I. I. Didenkulova, N. Zahibo, and E. N. Pelinovsky, *Reflection of long waves from a nonreflecting bottom profile*, Fluid Dyn., 43 (2008), pp. 590–595.

[6] K. Ko and H. H. Kuehl, *Korteweg-de Vries Soliton in a Slowly Varying Medium*, Phys. Rev. Let., 40 (1978), pp. 233–236.

[7] G. K. Pedersen, *Fully nonlinear boussinesq equations for long wave propagation and run-up in sloping channels with parabolic cross sections*, Natural Hazards, 84 (2016), pp. 599–619. DOI:10.1007/s11069-016-2448-0.

[8] C. E. Synolakis, *The run-up of solitary waves*, J. Fluid Mech., 185 (1987), pp. 523–545.

[9] W. C. Thacker, *Some exact solutions to the nonlinear shallow-water wave equations*, J. Fluid Mech., 107 (1981), pp. 499–508.